Enhanced Sensing of Weak Anharmonicities through Coherences in Dissipatively Coupled Anti-PT Symmetric Systems

Jayakrishnan M. P. Nair, Debsuvra Mukhopadhyay, and G. S. Agarwal

Phys. Rev. Lett. **126**, 180401 — Published 7 May 2021

DOI: 10.1103/PhysRevLett.126.180401

Enhanced sensing of weak anharmonicities through coherences in dissipatively coupled anti-PT symmetric systems

Jayakrishnan M. P. Nair,[1,*] Debsuvra Mukhopadhyay,[1,†] and G. S. Agarwal[1,2,‡]

[1]*Institute for Quantum Science and Engineering, Department of Physics and Astronomy, Texas A&M University, College Station, TX 77843, USA*

[2]*Department of Biological and Agricultural Engineering, Texas A&M University, College Station, TX 77843, USA*

(Dated: February 26, 2021)

In the last few years, the great utility of exceptional points (EPs) in sensing linear perturbations has been recognized. However, physical systems are inherently anharmonic and macroscopic physics is most accurately described by nonlinear models. Considering the multitude of semiclassical and quantum effects ensuing from nonlinear interactions, the sensing of anharmonicities is a prerequisite to the primed control of these effects. Here, we propose an expedient sensing scheme relevant to dissipatively coupled anti Parity-Time (anti PT) symmetric systems and customized for the fine-grained estimation of anharmonic perturbations. The sensitivity to anharmonicities is derived from the coherence between two modes induced by a common vacuum. Owing to this coherence, the linear response acquires a pole on the real axis. We demonstrate how this singularity can be exploited for the enhanced sensing of very weak anhamonicities at low pumping rates. Our results are applicable to a wide class of systems, and we specifically illustrate the remarkable sensing capabilities in the context of a weakly anharmonic Yttrium Iron Garnet (YIG) sphere interacting with a cavity via a tapered fiber waveguide. A small change in the anharmonicity leads to a substantial change in the induced spin current.

In the modern world with proliferating technological advances, sensing is of fundamental importance, with far-reaching applications [1–5] across various scientific disciplines, with adoptions as particle sensors, motion sensors and more. Both semiclassical and quantum phenomena provide us with a wide range of techniques to attain remarkable efficacy in sensing operations. Over the past decade, non-Hermitian degeneracies known as exceptional points (EPs) in [6–10] have rendered a new avenue to engineer augmented response in an open quantum system [11–20], particularly in PT-symmetric systems with a commensurate gain-loss profile [21–24]. Some recent experiments include the demonstration of enhanced sensitivity in microcavities near EPs [11] and the observation of higher-order EPs in a coupled-cavity arrangement [12]. While this is a truly remarkable development and has acquired a lot of traction, these methodologies are customized to sense only linear perturbations. One would like to examine the possibilities of newer sensing techniques, which could be tapped for the detection of anharmonic perturbations.

In this letter, we demonstrate a new physical basis for the enhanced sensing of nonlinearities without utilizing a commensurate gain-loss profile. We consider dissipatively coupled systems where the coupling is produced via interaction with the vacuum of the electromagnetic field [25]. Recently, anti-PT symmetric systems have been considered for the sensing of linear perturbations [26]. Our scheme, on the other hand, focuses on the sensing of mode anharmonicities. Dissipatively coupled systems have the novel property that vacuum induces coherence between two modes. The phenomenon of vacuum induced coherence (VIC) has been the subject of intense activity [27–41] with applications ranging from heat engines [31], nuclear gamma ray transmission [37] to photosynthesis [38] and molecular isomerization in vision [41]. In a linear system with strong VIC, one of the eigenvalues characterizing its dynamics moves to the real axis. We demonstrate the great utility of this key property to the sensing of extremely weak nonlinearities which are, otherwise, difficult to detect. This new paradigm is applicable generally to a wide class of systems encountered across various scientific disciplines. Examples include quantum dots coupled to plasmonic excitations in a nanowire [42], superconducting transmon qubits [43], quantum emitters coupled to metamaterials [27–29, 44], optomechanical systems [45], hybrid magnon-photon systems [46] and more.

We show explicit results on enhanced sensing by employing the VIC paradigm in an anti-PT symmetric configuration to the detection of very weak magnetic nonlinearities in a YIG sphere coupled to a cavity [46–59]. This system is specifically chosen in view of the ongoing experimental activities. Dissipative coupling using YIGs has been observed in a multitude of settings, involving, for instance, a Fabry-perot cavity [46] or a coplanar waveguide [47]. Note that under most circumstances, weak nonlinearities of the order of nHZ would require immense drive power to be detected in experiments. However, a dissipatively coupled system affords a prodigious response in the magnetization of the YIG which goes up spectacularly with the weakening strength of nonlinearity. That this response is strongly sensitive to variations in the strength of anhamonicity underpins the utility of our scheme in sensing applications.

We start off by considering the general model for a two-mode anharmonic system, which is pertinent to a wide range of physical systems. This is characterized by a Hamiltonian

$$\begin{aligned} H/\hbar = \omega_a a^\dagger a + \omega_b b^\dagger b + g(ab^\dagger + a^\dagger b) \\ +U(b^{\dagger 2}b^2) + i\Omega(b^\dagger e^{-i\omega_d t} - be^{i\omega_d t}), \end{aligned} \tag{1}$$

where ω_a and ω_b denote the respective resonance frequencies of the uncoupled modes a and b, and g constitutes the co-

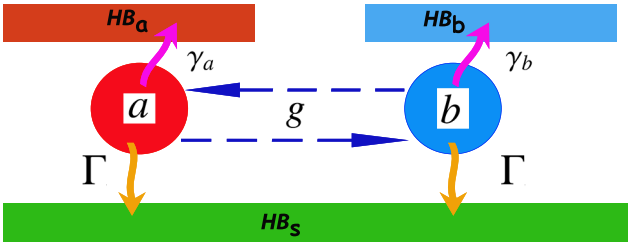

FIG. 1: Schematic of a general two-mode system dissipatively coupled through a waveguide. $\gamma_{a(b)}$ and Γ describe decay into the surrounding (local heat bath) and coupling to the fiber (shared bath) respectively.

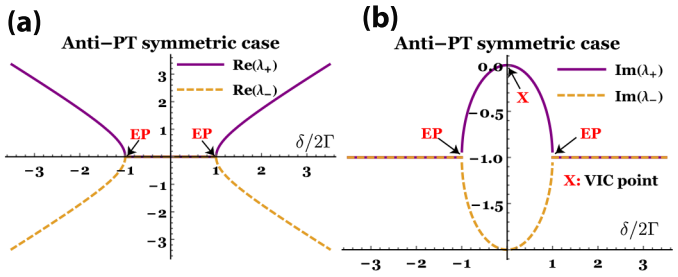

FIG. 2: a) Eigenfrequencies and b) linewidths for an anti-PT symmetric system, plotted against the detuning, with γ_0 set equal to 0. While EPs emerge at $\delta = \pm 2\Gamma$, the VIC-induced linewidth suppression (designated as X) corresponds to $\delta = 0$.

herent hermitian coupling between them. The parameter U is a measure of the strength of anharmonicity intrinsic to the mode b, which is driven externally by a laser at frequency ω_d. The quantity Ω represents the Rabi frequency. In addition, these modes could be interfacing with a dissipative environment. Dissipative environments in an open quantum system fall roughly under two classifications - one, where the modes are coupled independently to their local heat baths, and another, where a common reservoir interacts with both, as depicted in figure (1).

A complete description of the two-mode system, in terms of its density matrix ρ, is provided by the master equation [25]

$$\frac{\mathrm{d}\rho}{\mathrm{d}t} = -\frac{i}{\hbar}[H,\rho] + \gamma_a \mathscr{L}(a)\rho + \gamma_b \mathscr{L}(b)\rho + 2\Gamma\mathscr{L}(c)\rho, \qquad (2)$$

where γ_a and γ_b are, respectively, the intrinsic damping rates of the modes, induced by coupling with their independent heat baths. The parameter Γ introduces coherences, and the Liouvillian operator $\mathscr{L}$ is defined by its action $\mathscr{L}(\sigma)\rho = 2\sigma\rho\sigma^\dagger - \sigma^\dagger\sigma\rho - \rho\sigma^\dagger\sigma$. Assuming symmetrical couplings of the modes to the common reservoir we have the relation $c = \frac{1}{\sqrt{2}}(a + e^{i\phi}b)$. Here $\phi = 2\pi L/\lambda_0$ embodies the phase difference between the two couplings, where λ_0 is the resonant wavelength and L the spatial separation between a and b. Granted that the wavelength of the resonant mode to be much bigger than the spatial separation, we approximate $\phi \approx 0$. The mean value equations for a and b are obtained to be

$$\begin{pmatrix}\dot{a}\\ \dot{b}\end{pmatrix} = -i\mathscr{H}\begin{pmatrix}a\\ b\end{pmatrix} - 2iU(b^\dagger b)\mathscr{R}\begin{pmatrix}a\\ b\end{pmatrix} + \Omega e^{-i\omega_d t}\begin{pmatrix}0\\ 1\end{pmatrix}, \qquad (3)$$

where $\mathscr{H} = \begin{pmatrix}\omega_a - i(\gamma_a+\Gamma) & g - i\Gamma\\ g - i\Gamma & \omega_b - i(\gamma_b+\Gamma)\end{pmatrix}$, $\mathscr{R} = \begin{pmatrix}0 & 0\\ 0 & 1\end{pmatrix}$, and the notation $\langle . \rangle$ has been dropped for conciseness. In dealing with the nonlinear term, we have taken recourse to the mean-field approximation $\langle \mathscr{X}_1\mathscr{X}_2\rangle = \langle \mathscr{X}_1\rangle\langle \mathscr{X}_2\rangle$ for any two operators $\mathscr{X}_1$ and $\mathscr{X}_2$. A canonical transformation of the form $(a,b) \to e^{-i\omega_d t}(a,b)$ stamps out the time dependence on the final term in (3) and translates $\mathscr{H}$ to $\mathscr{H}^{(d)} = \mathscr{H} - \omega_d \mathbb{1}$ without tampering with the nonlinear term, where $\mathbb{1}$ is the 2×2 identity matrix. This transformation takes us to the frame of the applied laser frequency.

Before proceeding with a generalized treatment, let us first deconstruct the linear dynamics, i.e. when U is dropped. Defining $\delta = \omega_a - \omega_b$ and the mode detunings $\Delta_i = \omega_i - \omega_d$ $(i = a, b)$, we have the eigenvalues of $\mathscr{H}$ given by $\lambda_\pm = \frac{\omega_a+\omega_b}{2} - i(\gamma_0 + \Gamma) \pm \sqrt{(\delta/2 - i\gamma_{ab})^2 + (g - i\Gamma)^2}$, with $\gamma_0 = (\gamma_a + \gamma_b)/2$ and $\gamma_{ab} = (\gamma_a - \gamma_b)/2$. Contingent on the stability condition $\mathrm{Im}(\lambda_\pm) < 0$, which averts exponential amplification, the steady-state solutions for the mean values $\mathscr{O}^{(i)} = \langle O\rangle$ $(\mathscr{O}^{(i)} = \mathscr{A}, \mathscr{B}; i = a, b)$ would unfold as

$$\frac{\mathscr{A}}{\Gamma + ig} = \frac{\mathscr{B}}{i\Delta_a - \gamma_a - \Gamma} = \frac{\Omega}{(\omega_d - \lambda_+)(\omega_d - \lambda_-)}. \qquad (4)$$

Palpably, the linear response can diverge if one of the eigenvalues moves to the real axis. The feasibility of this property is explicated for a few special cases in the subsequent discussion.

The generic 2×2 matrix $\mathscr{H}$ encompasses two distinct subtypes: (i) coherently coupled systems with $\Gamma = 0$, and (ii) dissipatively coupled systems with $g = 0$. Two special symmetries can be realized within these folds, namely PT-symmetry (allowed by (i)), which obey $(\hat{PT})\mathscr{H}(\hat{PT}) = \mathscr{H}$, and anti-PT symmetry (allowed by (ii)), with $(\hat{PT})\mathscr{H}(\hat{PT}) = -\mathscr{H}$. An anti-PT symmetric realization of mode hybridization can be pinned down by the parameter choices $\gamma_{ab} = g = 0$, $\Delta_a = -\Delta_b = \delta/2$ and $\Gamma \neq 0$. Clearly, while the modes are oppositely detuned in character, both of them retain their lossy nature. Here, it makes sense to switch to the rotating frame of the laser, where $\mathscr{H}$ is substituted by $\mathscr{H}^{(d)}_{aPT} = \begin{pmatrix}\delta/2 - i(\gamma_0+\Gamma) & -i\Gamma\\ -i\Gamma & -\delta/2 - i(\gamma_0+\Gamma)\end{pmatrix}$. The shifted eigenvalues would be obtained as $-i(\gamma_0+\Gamma) \pm \sqrt{\delta^2/4 - \Gamma^2}$ for $|\delta/2| > \Gamma$ and $-i(\gamma_0+\Gamma) \pm i\sqrt{\Gamma^2 - \delta^2/4}$ (broken anti-PT) for $|\delta/2| < \Gamma$. The behavior of the real and imaginary parts of these eigenvalues is provided in figure 2 (a), (b). As long as the stability criterion is fulfilled, the responses in (4) are inversely related to $\det\left[\mathscr{H}^{(d)}_{aPT}\right] = (\omega_d - \lambda_+)(\omega_d - \lambda_-) = -[\delta^2/4 + \gamma_0(2\Gamma + \gamma_0)]$. The broken anti-PT phase brings in real singularities at $\delta = 0$

in the limit $\gamma_0 \to 0$, which is evidenced by the resonant inhibition in the imaginary part of λ_+, as marked by the point X in figure 2 (b). The extreme condition $\gamma_0 = 0$ holds when none of the modes suffers spontaneous losses to its independent surrounding, all the while interacting with the mediating reservoir. The point X distinguishes an especially long-lived resonance, which leads to a tremendous buildup in the steady-state amplitudes. We would demonstrate later how the inclusion of anharmonicity promptly regularizes the divergent linear response, with the nonlinear response being highly sensitive to variations in the strength of anharmonicity. This constitutes the bedrock of our sensing scheme.

Note that the point X in anti-PT symmetric systems is functionally analogous to the EP in PT-symmetric systems. The PT-symmetric configuration for coherently coupled systems is conformable with the parameter structure $\Delta = \gamma_0 = \Gamma = 0$. The constraint $\gamma_a = -\gamma_b = \gamma_{ab}$ implies that a loss in mode a must be offset by a commensurate gain in mode b. It follows that the transition point $|\gamma_{ab}| = g$, which defines the EP, introduces real singularities by quenching the linewidths to nought.

Next, we illustrate the importance of the condition $\mathrm{Im}(\lambda_+) \to 0$ in the context of the nonlinear response observed in the system. The nonlinear behavior depends on the intrinsic symmetry properties of the matrix $\mathscr{H}$. Specifically, the extraordinary response achievable in anti-PT symmetric models yields a convenient protocol for the fine-grained estimation of weak anharmonicity. We now consider a full treatment of Eq. (3) by factoring in the effect of U. In the rotating frame, upon setting $g = 0$ and choosing $\gamma_a = \gamma_b = \gamma_0$, this leads to the modified steady-state relations:

$$\begin{aligned} -(i\delta/2 + \gamma_0 + \Gamma)a - \Gamma b = 0, \\ -(-i\delta/2 + \gamma_0 + \Gamma)b - 2iU|b|^2 b - \Gamma a + \Omega = 0. \end{aligned} \tag{5}$$

Defining $\gamma = \gamma_0 + \Gamma$ and eliminating a, the intensity $x = |b|^2$ is found to satisfy a cubic relation

$$\frac{\beta^2}{\gamma^2 + (\delta/2)^2} x - \frac{2U\beta\delta}{\gamma^2 + (\delta/2)^2} x^2 + 4U^2 x^3 = I, \tag{6}$$

where $\beta = \Gamma^2 - \gamma^2 - (\delta/2)^2$ and $I = \Omega^2$. Eq. (6) can entail a bistable response under the condition $U\delta < 0$ and $\delta^2 > 12\gamma^2$. However, throughout this manuscript, we operate at adequately low drive powers to ward off bistable signature. Now, in the limit $\gamma_0 \to 0$ and $\delta \to 0$, β becomes vanishingly small, and the first two terms in Eq. (6) recede in importance, for a given Rabi frequency Ω. Consequently, in the neighborhood of $\delta = 0$, the response becomes highly sensitive to variations in U. To be more precise, for sufficiently low values of the detuning, the response mimics the functional dependence $x \approx (I/4U^2)^{1/3}$. A tenfold decrease in U, therefore, scales up the peak intensity of b by a factor of 4.64. In this context, it is useful to strike a correspondence with the sensitivity in eigenmode splitting around an EP which is typically employed in PT-symmetric sensing protocols [11, 12, 15]. For two-mode systems, where the EP is characterized by a square root singularity, this splitting $\delta\omega$ scales as the square root of the perturbation parameter ϵ implying a sensitivity that goes as $\left|\frac{\delta\omega}{\delta\epsilon}\right| \propto |\epsilon|^{-1/2}$. However, in our setup, the sensitivity to U in the response is encoded as $\left|\frac{\delta x}{\delta U}\right| \propto |U|^{-5/3}$.

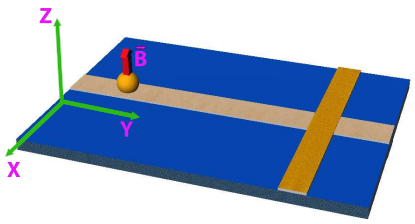

FIG. 3: Schematic of the cavity-magnonic setup. The microwave cavity, running transverse to the waveguide, interacts with the YIG via the transmission line. A static magnetic field aligned along the z-axis generates the Kittel mode in YIG.

The importance of the above result in the context of sensing is hereby legitimized for dissipatively coupled systems. Guided by the recent experiments on dissipatively coupled hybrid magnon-photon systems [46–52], we apply these ideas to the specific example of Kerr nonlinearity in a YIG sample [59]. However, the bulk of these works have restricted their investigations to the linear domain. Here, we transcend this restriction and study the nonlinear response to an external drive. We consider an integrated apparatus comprising a microwave cavity and a YIG sphere, both interfacing with a one-dimensional waveguide [49, 50], as depicted in figure 3. Owing to the nonexistent spatial overlap between the cavity and magnon modes, the direct coupling between them can be dropped. However, the interaction with the waveguide would engender an indirect coupling between them. In order to excite the weak Kerr nonlinearity of the YIG sphere, a microwave laser is used to drive the spatially uniform Kittel mode. The full Hamiltonian in presence of the external drive can be cast exactly in the form of Eq. (1), with b superseded by the magnonic operator m [59, 60].

As discussed earlier, the mediating effect of the waveguide is reflected as a dissipative coupling between the two modes, which instills VIC into the system. With the anti-PT symmetric choices $\Delta_a = -\Delta_m = \delta/2$, $\gamma_a = \gamma_b = \gamma_0$, and the redefinition $\gamma_0 + \Gamma = \gamma$, we recover Eq. (6) in the steady state, with the obvious substitution $b \to m$ and $x = |m|^2$ denoting the spin current response. We now expound the utility of engineering a lossless system in sensing weak Kerr nonlinearity. To that end, we zero in on the parameter subspace $\Gamma = \gamma = 2\pi \times 10$ MHz. Since $\beta = -\delta^2/4$, the contributions from the first two terms in Eq. (6) taper off as resonance is approached. As outlined earlier, we find that for all practical purposes, the nonlinear response can be approximated as $x \approx (I/4U^2)^{1/3}$ in the region $\delta/2\pi < 1$ MHz, which demonstrates its stark sensitivity to U. A lower nonlinearity begets a higher response, as manifested in figure 4 (a), where plots of x against δ are studied at differing strengths of the nonlinearity. Even at $D_p = 1\ \mu W$, we observe a significant enhancement in

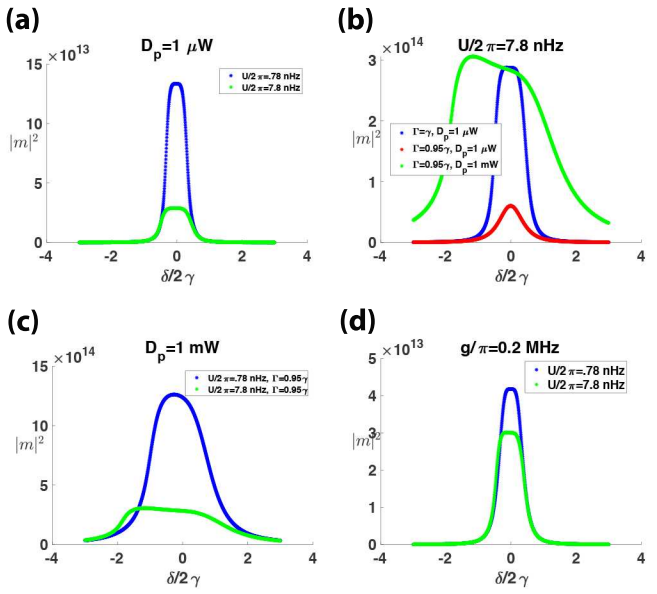

FIG. 4: a) The spin current plotted against δ at two different nonlinearities; b) spin currents away from the VIC condition, compared against the lossless scenario, at different drive powers- for ease of comparison, the blue and red curves have been scaled up by 10; c) contrasting responses observed at a drive power of 1 mW for two different strengths of nonlinearity; d) sensitivity for a nonzero coherent coupling g at $D_p = 1$ μW.

the induced spin current of the YIG around $\delta = 0$. The result is a natural upshot of the VIC-induced divergent response in an anti-PT symmetric system in the linear regime. Quite conveniently, the inclusion of nonlinearity dispels the seemingly absurd problem of a real singularity noticed in the linear case. If $\Gamma < \gamma$, a strong quenching in the response is observed, as depicted in figure 4 (b). The sensitivity to variations in U also incurs deleterious consequences. Nevertheless, we can counteract this decline by boosting the drive power. A drive power close to 1 mW can bring back the augmented response and the pronounced sensitivity to U (figure 4 (c)). By the same token, the introduction of coherent coupling g between the two modes prompts a decline in the sensitivity. The real singularity pertaining to a purely dissipative linear model is now replaced by a complex one, i.e., with a finite linewidth, bringing down the sharpness of the resonance and similarly, the sensitivity. Here, a tenfold depreciation in U barely generates an enhancement factor of 1.39 in the response, as illustrated in figure 4 (d). This is to be contrasted with the $g = 0$ case in figure 4 (a), where the magnification factor is 4.64 for an otherwise identical set of parameters. Propitiously, systems with zero coherent coupling were engineered in recent experiments [49, 50]. This mechanism can, thus, serve as an efficient tool to sense small anharmonicities present in a system.

The protocol hinges on the anti-PT symmetric character and

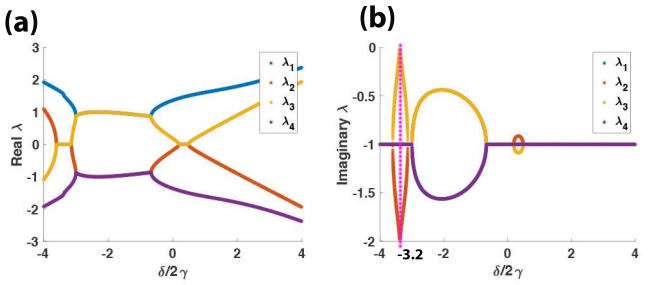

FIG. 5: a) Real and b) imaginary parts of the eigenvalues of $\mathscr{H}_{NL}$ at a drive power of 0.1 W.

eigenmodes of $\mathscr{H}$, which largely control the dynamics at low drive powers. At larger drive powers (~ 0.1 W), the nonlinear correction in (3) becomes important. This phenomenon can be understood by studying the modified spectroscopic character of the system in response to a weak probe field. The nonlinear effects can be encapsulated as time-varying fluctuations to the steady-state values, *viz.* $a(t) = a + \delta a(t)$, $b(t) = b + \delta b(t)$. By virtue of linearization [61], the dynamics of the fluctuations $\delta\xi = \left(\delta a(t) \;\; \delta b(t) \;\; \delta a^\dagger(t) \;\; \delta b^\dagger(t)\right)^T$ could be explained through a higher-dimensional Hamiltonian matrix,

$$\mathscr{H}_{NL} = \begin{pmatrix} -\frac{\delta}{2} - i\gamma & -i\Gamma & 0 & 0 \\ -i\Gamma & \tilde{\Delta} - i\gamma & 0 & 2Ub^2 \\ 0 & 0 & \frac{\delta}{2} - i\gamma & -i\Gamma \\ 0 & -2Ub^{*2} & -i\Gamma & -\tilde{\Delta} - i\gamma \end{pmatrix}, \qquad (7)$$

where $\tilde{\Delta} = \frac{\delta}{2} + 4U|b|^2$. The eigenvalues of this matrix, for the cavity-magnon setting, appear in figure 5. Strong anharmonicity alters the coherence properties of the system, as reinforced by the extreme linewidth narrowing observed now around $\frac{\delta}{2\gamma} = -3.2$ in figure 5 (b). Note that the nonlinear corrections stem from the matrix elements $2Ub^2$ and $-2Ub^{*2}$. Thus, the higher-dimensional eigensystem attains precedence over the linear model when the product $U|b|^2$ becomes comparable to Γ. However, in the event that $U|b|^2 \ll \Gamma$, the nonlinearity acts merely as a perturbation. It is precisely in this weakly anharmonic regime that our sensing proposal holds relevance.

In summary, we have proposed a dissipative test bed that shows enhanced sensitivity to Kerr nonlinearity of the mode, hence qualifying it as a prototypical agency to gauge the strength of anharmonic perturbations under optimal conditions. The sensitivity to anharmonicities can be traced down to the existence of a remarkably long-lived eigenmode of the linear system, characterized by a vanishing linewidth. The physical origin of this peculiar behavior lies in an effective coupling induced between the cavity and the magnon modes in the presence of a shared ancillary reservoir. Optimal results vis-à-vis the estimation of nonlinearity are obtained when VIC strongly dominates, i.e., when spontaneous emissions from the modes to the surrounding environments become negligible in comparison to the waveguide-mediated coupling. Higher drive

powers lead to new domains of VIC on account of strongly anharmonic responses. The precise implications of these new VICs would be a subject of future study. To provide numerical estimates, our analysis has been tailored to demonstrate a pronounced sensitivity in the context of magnonic excitations. Nonetheless, the essence of our assessment would be applicable to any two-mode nonlinear system.

ACKNOWLEDGMENTS

The authors gratefully acknowledge the support of The Air Force Office of Scientific Research [AFOSR award no FA9550-20-1-0366], The Robert A. Welch Foundation [grant no A-1243] and the Herman F. Heep and Minnie Belle Heep Texas A&M University endowed fund. GSA thanks Dr. C. M. Hu for discussions on the dissipative coupling and for sharing his data with us.

* jayakrishnan00213@tamu.edu
† debsosu16@tamu.edu
‡ girish.agarwal@tamu.edu

[1] E. Gil-Santos, D. Ramos, J. Martínez, M. Fernández-Regúlez, R. García, Á. San Paulo, M. Calleja, and J. Tamayo, Nature nanotechnology **5**, 641 (2010).
[2] J. Zhu, S. K. Ozdemir, Y.-F. Xiao, L. Li, L. He, D.-R. Chen, and L. Yang, Nature photonics **4**, 46 (2010).
[3] L. He, Ş. K. Özdemir, J. Zhu, W. Kim, and L. Yang, Nature nanotechnology **6**, 428 (2011).
[4] F. Vollmer and L. Yang, Nanophotonics **1**, 267 (2012).
[5] S. Forstner, S. Prams, J. Knittel, E. D. van Ooijen, J. D. Swaim, G. I. Harris, A. Szorkovszky, W. P. Bowen, and H. Rubinsztein-Dunlop, Phys. Rev. Lett. **108**, 120801 (2012).
[6] L. Chang, X. Jiang, S. Hua, C. Yang, J. Wen, L. Jiang, G. Li, G. Wang, and M. Xiao, Nature photonics **8**, 524 (2014).
[7] I. I. Arkhipov, A. Miranowicz, O. Di Stefano, R. Stassi, S. Savasta, F. Nori, and i. m. c. K. Özdemir, Phys. Rev. A **99**, 053806 (2019).
[8] W. Heiss, Journal of Physics A: Mathematical and Theoretical **45**, 444016 (2012).
[9] H. Xu, D. Mason, L. Jiang, and J. Harris, Nature **537**, 80 (2016).
[10] H. Cao and J. Wiersig, Rev. Mod. Phys. **87**, 61 (2015).
[11] W. Chen, Ş. K. Özdemir, G. Zhao, J. Wiersig, and L. Yang, Nature **548**, 192 (2017).
[12] H. Hodaei, A. U. Hassan, S. Wittek, H. Garcia-Gracia, R. El-Ganainy, D. N. Christodoulides, and M. Khajavikhan, Nature **548**, 187 (2017).
[13] Z. Xiao, H. Li, T. Kottos, and A. Alù, Phys. Rev. Lett. **123**, 213901 (2019).
[14] Z. Lin, A. Pick, M. Lončar, and A. W. Rodriguez, Physical review letters **117**, 107402 (2016).
[15] J. Wiersig, Phys. Rev. Lett. **112**, 203901 (2014).
[16] P.-Y. Chen and J. Jung, Phys. Rev. Applied **5**, 064018 (2016).
[17] M.-A. Miri and A. Alu, Science **363** (2019).
[18] X. Zhang, K. Ding, X. Zhou, J. Xu, and D. Jin, Phys. Rev. Lett. **123**, 237202 (2019).
[19] C. Zeng, Y. Sun, G. Li, Y. Li, H. Jiang, Y. Yang, and H. Chen, Optics express **27**, 27562 (2019).
[20] J. Wiersig, Phys. Rev. A **93**, 033809 (2016).
[21] C. M. Bender and S. Boettcher, Phys. Rev. Lett. **80**, 5243 (1998).
[22] C. M. Bender, M. Berry, and A. Mandilara, Journal of Physics A: Mathematical and General **35**, L467 (2002).
[23] C. M. Bender, D. C. Brody, and H. F. Jones, Phys. Rev. Lett. **89**, 270401 (2002).
[24] R. El-Ganainy, K. G. Makris, D. N. Christodoulides, and Z. H. Musslimani, Opt. Lett. **32**, 2632 (2007).
[25] G. S. Agarwal, in *Quantum Optics* (Springer, 1974) pp. 1–128.
[26] H. Zhang, R. Huang, S.-D. Zhang, Y. Li, C.-W. Qiu, F. Nori, and H. Jing, Nano Letters **20**, 7594 (2020).
[27] G. Agarwal, Physical Review Letters **84**, 5500 (2000).
[28] P. K. Jha, X. Ni, C. Wu, Y. Wang, and X. Zhang, Physical review letters **115**, 025501 (2015).
[29] E. Lassalle, P. Lalanne, S. Aljunid, P. Genevet, B. Stout, T. Durt, and D. Wilkowski, Physical Review A **101**, 013837 (2020).
[30] D. Kornovan, M. Petrov, and I. Iorsh, Physical Review A **100**, 033840 (2019).
[31] M. O. Scully, K. R. Chapin, K. E. Dorfman, M. B. Kim, and A. Svidzinsky, Proceedings of the National Academy of Sciences **108**, 15097 (2011).
[32] M. Kiffner, M. Macovei, J. Evers, and C. Keitel, in *Progress in Optics*, Vol. 55 (Elsevier, 2010) pp. 85–197.
[33] C. H. Keitel, Physical review letters **83**, 1307 (1999).
[34] P. Zhou and S. Swain, Physical Review A **56**, 3011 (1997).
[35] E. Paspalakis and P. Knight, Physical review letters **81**, 293 (1998).
[36] E. Paspalakis, C. H. Keitel, and P. L. Knight, Physical Review A **58**, 4868 (1998).
[37] K. P. Heeg, H.-C. Wille, K. Schlage, T. Guryeva, D. Schumacher, I. Uschmann, K. S. Schulze, B. Marx, T. Kämpfer, G. G. Paulus, *et al.*, Physical review letters **111**, 073601 (2013).
[38] K. E. Dorfman, D. V. Voronine, S. Mukamel, and M. O. Scully, Proceedings of the National Academy of Sciences **110**, 2746 (2013).
[39] M. O. Scully, Phys. Rev. Lett. **104**, 207701 (2010).
[40] A. A. Svidzinsky, K. E. Dorfman, and M. O. Scully, Phys. Rev. A **84**, 053818 (2011).
[41] A. Dodin and P. Brumer, The Journal of chemical physics **150**, 184304 (2019).
[42] H. Wei, Z. Li, X. Tian, Z. Wang, F. Cong, N. Liu, S. Zhang, P. Nordlander, N. J. Halas, and H. Xu, Nano letters **11**, 471 (2011).
[43] J. Koch, T. M. Yu, J. Gambetta, A. A. Houck, D. I. Schuster, J. Majer, A. Blais, M. H. Devoret, S. M. Girvin, and R. J. Schoelkopf, Phys. Rev. A **76**, 042319 (2007).
[44] I. Thanopulos, V. Yannopapas, and E. Paspalakis, Phys. Rev. B **95**, 075412 (2017).
[45] N. R. Bernier, L. D. Tóth, A. K. Feofanov, and T. J. Kippenberg, Phys. Rev. A **98**, 023841 (2018).
[46] M. Harder, Y. Yang, B. M. Yao, C. H. Yu, J. W. Rao, Y. S. Gui, R. L. Stamps, and C.-M. Hu, Phys. Rev. Lett. **121**, 137203 (2018).
[47] B. Bhoi, B. Kim, S.-H. Jang, J. Kim, J. Yang, Y.-J. Cho, and S.-K. Kim, Phys. Rev. B **99**, 134426 (2019).
[48] Y.-P. Wang, J. W. Rao, Y. Yang, P.-C. Xu, Y. S. Gui, B. M. Yao, J. Q. You, and C.-M. Hu, Phys. Rev. Lett. **123**, 127202 (2019).
[49] J. W. Rao, Y. P. Wang, Y. Yang, T. Yu, Y. S. Gui, X. L. Fan, D. S. Xue, and C.-M. Hu, Phys. Rev. B **101**, 064404 (2020).
[50] Y. Yang, Y.-P. Wang, J. W. Rao, Y. S. Gui, B. M. Yao, W. Lu, and C.-M. Hu, Phys. Rev. Lett. **125**, 147202 (2020).

[51] B. Yao, T. Yu, Y. Gui, J. Rao, Y. Zhao, W. Lu, and C.-M. Hu, Communications Physics **2**, 1 (2019).
[52] Y.-P. Wang and C.-M. Hu, Journal of Applied Physics **127**, 130901 (2020).
[53] A. Metelmann and A. A. Clerk, Phys. Rev. X **5**, 021025 (2015).
[54] W. Yu, J. Wang, H. Y. Yuan, and J. Xiao, Phys. Rev. Lett. **123**, 227201 (2019).
[55] X. Zhang, C.-L. Zou, L. Jiang, and H. X. Tang, Phys. Rev. Lett. **113**, 156401 (2014).
[56] Y. Tabuchi, S. Ishino, T. Ishikawa, R. Yamazaki, K. Usami, and Y. Nakamura, Phys. Rev. Lett. **113**, 083603 (2014).
[57] Y. Tabuchi, S. Ishino, A. Noguchi, T. Ishikawa, R. Yamazaki, K. Usami, and Y. Nakamura, Science **349**, 405 (2015).
[58] S. P. Wolski, D. Lachance-Quirion, Y. Tabuchi, S. Kono, A. Noguchi, K. Usami, and Y. Nakamura, Phys. Rev. Lett. **125**, 117701 (2020).
[59] Y.-P. Wang, G.-Q. Zhang, D. Zhang, X.-Q. Luo, W. Xiong, S.-P. Wang, T.-F. Li, C.-M. Hu, and J. Q. You, Phys. Rev. B **94**, 224410 (2016).
[60] J. M. P. Nair, Z. Zhang, M. O. Scully, and G. S. Agarwal, Phys. Rev. B **102**, 104415 (2020).
[61] Z. Zhang, M. O. Scully, and G. S. Agarwal, Phys. Rev. Research **1**, 023021 (2019).